# Using Positive Muons to investigate High Temperature Superconductors

S.L. Lee

Physik Institut der Universität Zurich, Winterthurerstrasse 190, GH 8057 Zurich, Switzerland.

## Abstract

A short review is presented of the application of the muon-spin rotation ($\mu^+$SR) technique to the investigation of high-temperature (HTC) superconducting materials. An elementary discussion of the mixed state in extreme type II superconductors is given, and it is shown how $\mu^+$SR may be used to measure the probability distribution p(B) of the internal magnetic fields in this state. Different methods for extracting the superconducting penetration depth $\lambda$ from p(B) are described. Measurements of the temperature dependence of $\lambda$ are briefly discussed, and a review is given of some recent measurements and theories concerning 'universal' trends of $\lambda$ the HTC materials. Recent $\mu^+$SR measurements in $Bi_2Sr_2CaCu_2O_8$ (BSCCO) are presented, which provide strong evidence for flux lattice melting in this material.

## 1. Introduction

Over the past decade the use of muons to investigate problems in solid state physics has become powerful and established technique (1, 2). This is particularly true in the field of superconductivity where the muon has proved to be a unique microscopic probe of the magnetic properties. While muon techniques have been applied successfully to the study of magnetic ordering in families of superconducting materials, especially in the high temperature (HTC) superconductors (see e.g. (2)), it is on the investigation of the superconducting state itself that I shall concentrate.

The muon spin rotation ($\mu^+$SR) technique provides a sensitive measure of microscopic field distribution inside a type-II superconductor, which in turn is related to the magnetic penetration depth, $\lambda$; this is one of the fundamental lengths of a superconductor, and is related to the superconducting order parameter. By using $\mu^+$SR to measure $\lambda$ as a function of temperature it might therefore be possible to investigate the pairing mechanism of the superconducting state. The details of the microscopic flux distribution itself is also of great interest, particularly

in view of some of the exotic magnetic phases proposed by recent theories for HTC systems (3) . Here I would like to discuss the application of $\mu^+$SR-technique to HTC research.

The discussion is organised as follows: In Section 2 I shall review some basic aspects of the mixed state in type II superconductors, and how we may utilise the $\mu^+$SR-technique to investigate the microscopic field distribution. In Section 3 the measurement of the magnetic penetration depth will be discussed, for arbitrary geometry in an anisotropic superconductor; the temperature dependence will also be briefly considered. In Section 4 trends of the superconducting properties within families of HTC materials will be discussed, including some recent results and ideas. The application of $\mu^+$SR to the investigation novel vortex structures is discussed in Section 5, together with some recent results which give evidence for flux-lattice melting. A summary is presented in Section 6.

## 2. Probing the mixed state with muons

In the mixed state of a type-II superconductor, for applied fields larger than the lower critical field $H_{c1}$, flux enters the bulk in the form of quantised lines of flux (see e.g. (4)). Each flux-line carries one quantum of flux $\Phi_0$ = h/2e and consists of a core of normal electrons around which there is a vortex-like flow of supercurrents. Such a vortex line is shown schematically in Fig.1(a), where two of the important lengths of the superconducting state have also been indicated; the first is the temperature-dependent superconducting coherence length $\xi$((T), which may loosely be thought of as the distance over which the superconducting wavefunction $\psi$(r) can fall to zero, and effectively defines the dimensions of the normal core. The second is the magnetic penetration depth $\lambda$(T), which is a measure of the distance over which the circulating supercurrents may screen a magnetic field, and thus gives the spatial extent of the isolated flux-line. As the applied field is increased, so is the internal density of flux-lines, so that they begin to overlap. In this case the field no longer falls to zero between flux-cores, as shown Fig.1(b). Due to the mutual repulsion between flux-lines they form a regular Abrikosov-lattice of plane spacing d, so that the internal flux-density B= $\phi_o/d^2$. At low temperatures HTC superconductors are characterised by $\lambda(0)\geq 1300$Å and $\xi(0)\leq 30$Å, so that the Ginzburg-Landau parameter $\kappa = \lambda/\xi >> 1$; such materials are normally described as extreme type-II superconductors. For such a system the finite core size only becomes important for very high flux-densities, at which the cores

themselves begin to overlap. Thus, for a very large range of fields $H_{c1}$ << H << $H_{C2}$, the flux distribution over most of space is determined largely by λ.

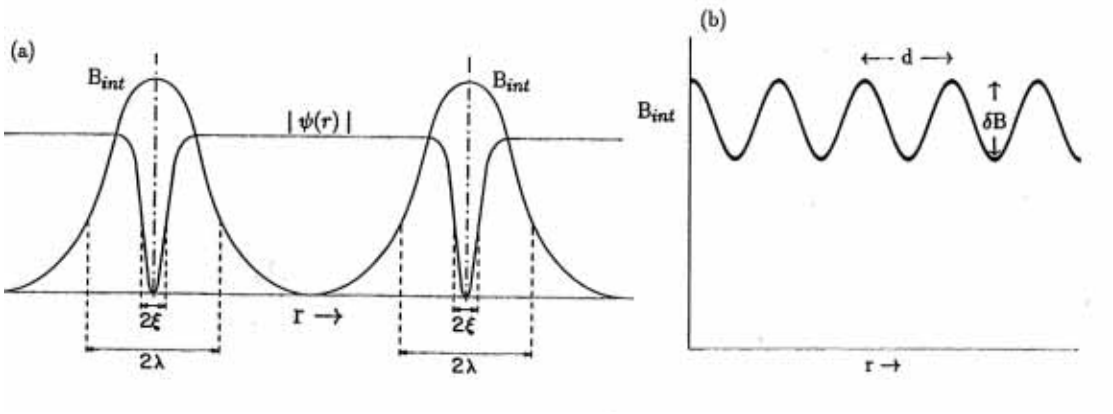


Figure 1: The structure of flux-lines in the mixed state (a) $H_{ext}$ ~ $H_{c1}$, and (b) $H_{c1}$, << $H_{ext}$ << $H_{c2}$, where a lattice of period d exists with a field contrast δB = $B_{max}$-$B_{min}$.

In the $\mu^+$SR-technique, highly spin-polarised muons are brought to rest in a sample which sits in a magnetic field $H_{ext}$ directed perpendicular to the muon spin. The muons then undergo Larmor precession in the local internal magnetic field $B_{int}$ at an angular frequency $\omega = \gamma_\mu B_{int}$, where $\gamma_\mu = 2\pi \times 1.36 \times 10^8$ Hz $T^{-1}$. The evolution with time of the muons may be measured by the detection of positrons which are emitted preferentially along the muon-spin direction during the decay of the muon, which has a mean lifetime of $\tau_\mu$ = 2.2μs. (For a more detailed discussion see for example (1)). A typical spectrum from such an experiment is shown Fig.2, where the positron detector output is shown , as a function of time. One can clearly see the oscillations due to muon-spin precession superimposed on the exponential muon decay. In general the observed spectrum may be described by the following function:

$$N(\theta, t) = N_o \exp(-t/\tau_\mu)[1 + AR(t)\cos(\omega t + \theta)] + b \qquad (1)$$

where No is the normalisation constant, A is the precession amplitude, θ is the initial phase, b is a constant background and ω and $\tau_\mu$ are as defined above. The relaxation function R(t) describes the damping of the precession signal, which in the mixed state arises from the distribution of internal fields B(r) around the average internal field $B_{av} = \langle B(r) \rangle$, where $\langle\rangle$ denotes the spatial average. Thus R(t) contains information about the internal field distribution of the vortex structure. This damping of the signal amplitude is readily observable in Fig.2(a). If one divides out the exponential decay from Eq.1 and performs a Fourier transform of the

data using some suitable technique, then one obtains the probability distribution p(B) of the internal field, which has a form determined by the details of the vortex structure. Such a p(B) for an idealised triangular lattice of vortex-lines is shown in Fig.2(b), and its details may be related to the spatial distribution B(r) (5). In particular the long "tail" at fields higher than the applied arises from regions close to the vortex cores. Thus one may investigate the field distribution arising from different vortex arrangements in the mixed state by measuring the $\mu^+$SR-lineshapes (6, 7).

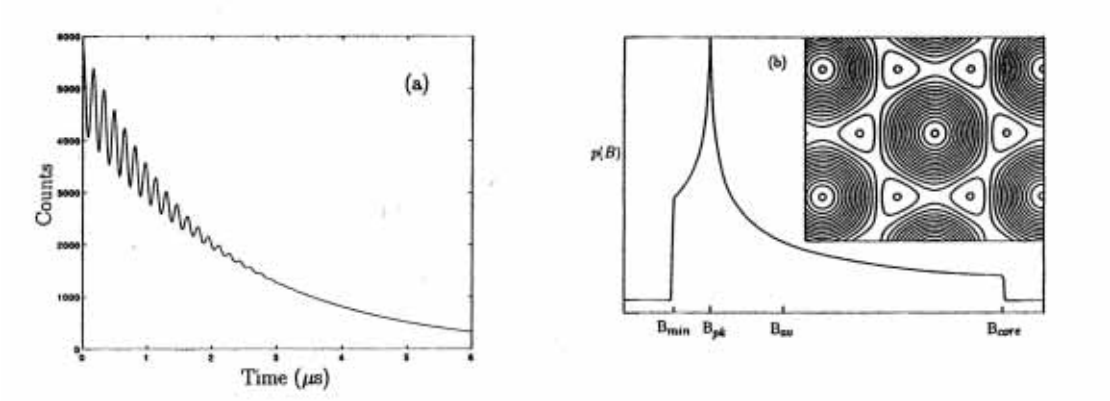


Figure 2: (a) A typical $\mu^+$SR time spectrum obtained from a superconductor in the mixed state. (b) Probability distribution p(B) for an ideal triangular vortex-line lattice. The inset shows the field contour plot of the corresponding lattice.

## 3. Measurement of the magnetic penetration depth λ

For an isotropic type II superconductor in the 'clean limit' (4) the magnetic penetration depth may be determined from:

$$\frac{1}{\lambda(0)} = \frac{\mu_o e^2 n_s(0)}{m^*}, \qquad (2)$$

where $n_s(0)$ is the density of the superfluid pairs at zero temperature and m* is the effective mass of the superconducting pairs. Due to the short coherence length in HTC materials Eq.2 should be a good description of λ. Thus λ is directly related to the superconducting charge carrier density and its temperature dependence provides important information on the pairing mechanism (4, 8, 9). λ(T) may often be described by the empirical formula:

$$\lambda(T) = \lambda(0)/(1 - t^n)^{1/2} \quad (T) \qquad (3)$$

where $t = T/T_c$ is the reduced temperature. Setting n =4 gives the two-fluid model (4), which for extreme type-II superconductors (κ>1)

represents a good approximation of the temperature dependence of an s-wave superconductor in the limit of strong coupling (8).

It has long since been realised that magnetic resonance methods can be used to measure directly the penetration depth of extreme type-II superconductors (10). More recently the analysis has been extended to describe the case of an anisotropic high-s system such as the HTC cuprates (11, 12, 13, 14, 15). The penetration depth $\lambda$ may be obtained from the second moment (linewidth) $\langle \Delta B^2 \rangle$ of the field distribution p(B), which in general may be written as the sum over reciprocal lattice-vectors G of the Fourier component of the internal magnetic field:

$$\left\langle \Delta B^2 \right\rangle = \sum_{G \neq 0} h(G) \,. \tag{4}$$

In the HTC cuprates, for the simple geometry of the applied field $H_{ext}$ parallel to the crystallographic ĉ-direction, this has been calculated to give

$$\left\langle \Delta B^2 \right\rangle = \frac{0.00371 \Phi_0^2}{\lambda^4} \tag{5}$$

for a triangular lattice when $H_{c1} << H_{ext} << H_{c2}$ (11, 12). Thus for a very wide range of fields the second moment is independent of field, and Eq.5 may be used to evaluate $\lambda$ directly. The conduction properties of HTC materials are anisotropic and have roughly uniaxial symmetry, so two principal values of the effective mass must be considered, $m^*_{ab}$ and $m^*_c$; these describe the supercurrents flowing parallel and perpendicular to the ab-planes (copper-oxide planes) respectively. For an arbitrary angle $\theta$ of the applied field to the ĉ-direction, the effective penetration depth must then be described by a tensor relation (13). It has been shown that within the London approximation one may describe a uniaxial superconductor for arbitrary field orientation by

$$\left\langle \Delta B^2 \right\rangle(\theta) = \left\langle \Delta B^2 \right\rangle(0)\left[\cos^2(\theta) + \gamma^{-2} \sin^2(\theta)\right] \tag{6}$$

where $\langle \Delta B^2 \rangle(0)$ is given by Eq.5 and $\gamma = (m_c/m_{ab})^{1/2} = \lambda_c/\lambda_{ab}$ is the anisotropy ratio (14, 13, 15). Eq.6 was found to be a good description of the angular-dependence of $\langle \Delta B^2 \rangle(0)$ in $YBa_2Cu_3O_{7-\delta}$ (YBCO), giving a value of $\gamma = 5$ (14). However, for the highly anisotropic material $Bi_2Sr_2CaCu_2O_8$ (BSCCO) such a description was found to be inappropriate, probably due to the quasi-2D nature of the flux-structure (16) (Fig.3). To calculate $\langle \Delta B^2 \rangle$ for polycrystalline or powder samples an average must be taken over all the possible crystal orientations. It has been shown that for a powder sample with an anisotropy ratio $\gamma \geq 5$, $\langle \Delta B^2 \rangle$ depends only on $m^*_{ab}$ and may be written as

$$\left\langle \Delta B^2 \right\rangle = \frac{0.00371 F \Phi_0^2}{\lambda_{ab}^4} \qquad (7)$$

where F≈ 0.44 (12). Thus the penetration depth $\lambda_{ab}$ due to the in-plane currents may be measured from polycrystalline samples without a precise knowledge of $\gamma$.

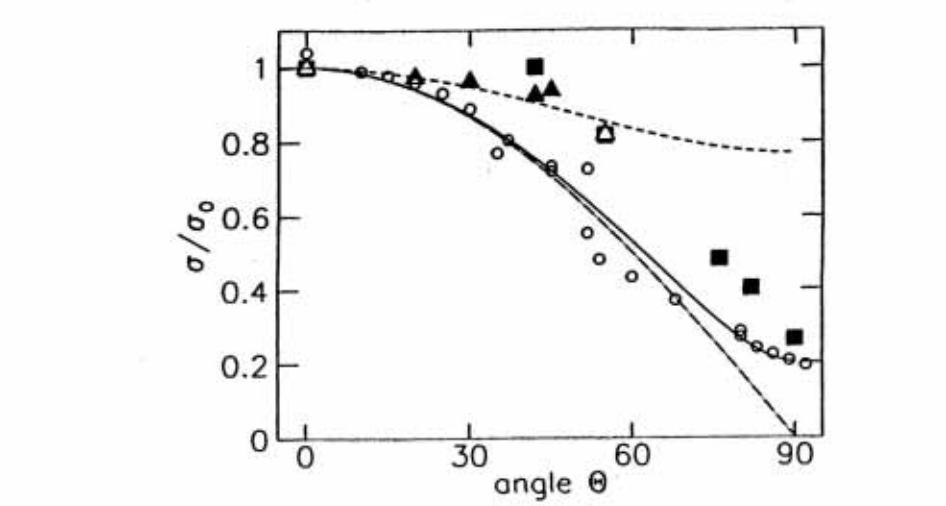


Figure 3: Angular-dependence of the muon-depolarisation rate a (a) in single-crystal YBCO (open circles) and (b) in single-crystal BSCCO (triangles, squares). The solid-line is a fit to the YBCO data to Eq.6, giving a $\gamma$ = 5. This model could not be used to describe the angular-dependence of the much more anisotropic BSCCO ($\gamma \geq 100$); the short and long dashed line corresponds to $\gamma \approx 1$ and $\gamma \approx \infty$ respectively (taken from ref. (16)).

The $\mu^+$SR-technique has proved to be an indispensable and reliable tool with which to measure the penetration depths of HTC materials. This has allowed systematic trends of the superconducting condensate density within families of materials and also to investigate 'universal' trends between different families (see Section 4). In practice for HTC systems the observation of probability distributions p(B) resembling Fig.2(b) are rare, due to a variety of factors. Imperfections of the vortex lattice due to random pinning may have the effect of convoluting this lineshape with a Gaussian, which smears out the van Hove singularity (11, 5), while demagnetisation effects may cause significant distortions of the spectra from polycrystalline samples (see e.g. (17)). For a great many cases the observed spectra are in fact found to be approximately Gaussian. It follows that in the $\mu^+$SR time-spectra the relaxation function R(t) of Eq.1 may also be approximated by a Gaussian

$$\mathrm{R(t)} = \exp\left( \frac{-\sigma^2 \mathrm{t}^2}{2} \right), \qquad \sigma = \gamma_\mu \left\langle \Delta \mathrm{B}^2 \right\rangle^{1/2} \qquad (8)$$

By this means the $\lambda$ may be extracted by fitting Eq.1 to the raw $\mu^+$SR time spectrum. Despite the apparent ease with which values for $\lambda$ may be extracted from $\mu^+$SR measurements, there are several considerations which should be taken into account. Firstly, for a vortex-line lattice the effects of lattice imperfection may cause a significant broadening of the observed $\langle \Delta B^2 \rangle$ leading to an underestimate of $\lambda$ (11, 5). In general, therefore, the values of $\lambda$ obtained from $\mu^+$SR should be considered as a lower limit. However, for the case of a close to ideal lineshape such as Fig.2(b) the long tail towards high-field values has a low probability p(B). For finite statistics not all of this tail will be observable above the experimental noise, leading to an incomplete spectrum. This apparent shortening of the tail will lead to an overestimate of $\lambda$. In such cases it is better to extract $\lambda$ from the distance $B_{pk}$-$B_{av}$, where $B_{pk}$ is the peak field of p(B) and $B_{av}$, is the average internal field, which may be determined from an independent method such as magnetisation measurements (see e.g. (18)). In highly anisotropic superconductors such as BSCCO the flux-structure may be quasi-2D (19), in which case random-pinning or thermally-induced disorder may cause a narrowing of the linewidth (20, 7, 21, 22), which can again lead to an overestimate of $\lambda$ if a only simple interpretation of the lineshape is made.

The experimental results regarding $\lambda(T)$ are still somewhat inconclusive. While the two-fluid model has been found to be a good description of the data in highly-oxygenated ceramic samples of YBCO (23), in ceramic $YBa_2Cu_4O_8$ and BSCCO the behaviour was found to be more BCS-like (weak-coupling) (24). A recent study of the exponent n in Eq.3 as a function of $\delta$ in $YBa_2Cu_3O_{7-\delta}$ has shown a systematic variation, with values ranging from $n \approx 2$ at low oxygen contents to $n \approx 4$ for well oxygenated samples (25). In general the situation may be complicated due to the influence of other factors on the measured second moments, as discussed above. Recent results in single-crystal BSCCO suggest that in that system thermal fluctuations of the vortex-positions may have a significant affect on the measured $\langle \Delta B^2 \rangle$, particularly at high fields (18, 7, 16, 22).

## 4. 'Universal' relations and trends in HTC materials

There have been many studies of the $\mu^+$SR relaxation rate $\sigma$ in both HTC and other extreme type-II materials (see e.g. (26) and references therein). In particular Uemura et al. performed a systematic study of the

low-temperature value of $\sigma$ for a large range of doped HTC materials. It was found that for all systems studied there was a common empirical relation between the transition temperature $T_c$ and the zero-temperature relaxation rate $\sigma(0)$; such a diagram is shown in Fig.4 and is known the 'Uemura plot' (27). Using Eqns. 2, 5 and 8 it can be seen that $\sigma(0) \propto n(0)/m^*_{ab}$ , so the Uemura plot effectively shows the dependence of $T_c$ on the condensate density. As the carrier doping is increased $T_c$ increases up to a maximum value $T^m_c$ and then saturates, and is eventually suppressed for higher doping levels. The initial rise of $T_c$ is common to all families of materials, but each family saturates at a different $T^m_c$. Such a relation provides an important testing ground for theoretical models which attempt to account for high-temperature superconductivity. For instance, it has been argued that the specific dependence of $T_c$ on $\sigma$ cannot be accounted for within the framework of weak-coupling BCS theory (27).

A phenomenological theory has recently been proposed to describe the Uemura plot (26). A parabolic maximum of $T_c$ close to the optimum condensate density $\sigma_m(0)$ is assumed which leads to the following scaling form

$$\overline{T}_c = 2\overline{\sigma}(1 - \overline{\sigma}/2), \quad \overline{T}_c = T_c / T_c^m, \quad \overline{\sigma} = \sigma(0) / \sigma_m(0) \ . \qquad (9)$$

In this way a given family forms a unique branch, which is characterised by $T_m$ and $\sigma_m(0)$. When the data for various families are plotted in this way they are found to lie on a single curve (Fig.4(b)). By assuming such an empirical relation, quantitative predictions may be made about thermodynamically related variables such as the pressure and isotope coefficients, where remarkable agreement is found with measured values (26, 28).

Recent $\mu^+$SR measurements on the thallium-based system $Th_2Ba_2CuO_{6+\delta}$ have extended the Uemura, plot well into the 'overdoped' region ($\sigma(0) > \sigma_m(0)$), where remarkably a reduction of $\sigma(0)$ is observed as the hole doping is increased beyond the optimum (29, 30). For this system in the regime $\sigma(0) > \sigma_m(0)$ the Uemura plot is no longer parabolic, but curls back on itself and extrapolates back to the origin, forming a 'fly-wing'. Several suggestions have been made to account for this apparent decrease of the superconducting carrier density which occurs despite an increase in the density of normal charge carriers. This behaviour has been attributed by ref. (29) to pair-breaking scattering processes which reduce the effective condensate density. A recent theory by ref. (31) describes the observed behaviour in terms of the Bose-Einstein condensation of a charged Bose gas with a strongly screened Coulomb repulsion. In this scenario it is the finite extent of the bosons which

gives rise to some critical density, above which they become immovable and $T_c$ -> 0. An interpolation between the dilute ideal Bose-gas regime and the dense regime gives the required behaviour. It seems clear that these and future $\mu^+$SR measurements will provoke further theoretical ideas which may be important to the detailed understanding of the superconducting state in the HTC materials.

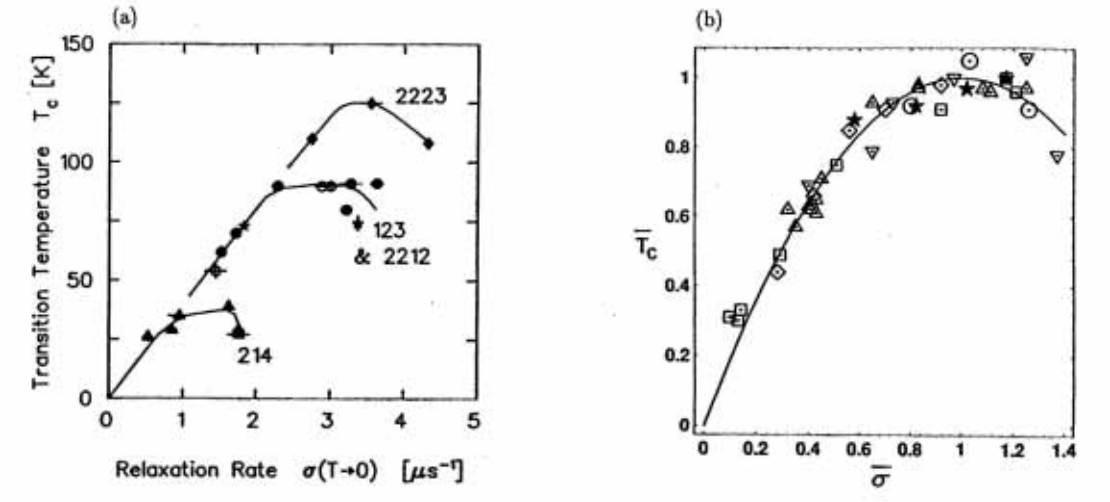


Figure 4: (a) The Uemura plot for various families of HTC superconductors. Details of the data shown may be found in ref. (27). (b) The data for various families rescaled according to Eq.9. The reader is referred to ref. (26) for details of the materials represented in the plot. Axis symbols are as defined in the text.

## 5. Microscopic observation of flux-lattice melting

The HTC superconductors have several properties which distinguish them from conventional low-$T_c$ systems: these include a very short coherence lengths $\xi$, high transition temperature $T_c$, and large anisotropy $\gamma$. The combination of these not unrelated properties leads to the possible occurrence of flux-vortex structures in the mixed state other than a regular Abrikosov-lattice, and also of transitions between these phases (3, 32, 33, 34, 19). In particular the existence of a melting-line $B_m(T)$ in the field-temperature (B-T) phase diagram has been the subject of much experimental effort (see e.g. (7, 35, 36, 37, 38, 39)). Such a transition involves a change from a 'vortex-solid' to a 'vortex-liquid', and is made more likely in HTC materials because (i) high thermal energies are accessible, (ii) the shear modulus $c_{66}$ of the flux solid is made small due to the high value of the Ginzburg-Landau parameter $\kappa$ and (iii) the high value of the anisotropy parameter $\gamma$ allows the possibility of enhanced quasi-2D fluctuations (33, 34, 32). Bulk measurements such as magnetisation and

resistivity reveal the presence of an irreversibility-line $B_{irr}$, below which hysteretic behaviour is observable, and attempts have been made to identify such a line with the microscopic melting-line (37, 38, 39). However, until recently clear evidence on a microscopic scale for vortex melting was not available. As discussed in Section 2, $\mu$SR is a very useful probe of the microscopic field distribution p(B) inside the mixed state, and as such may be used to measure changes of vortex structure. $\mu$SR measurements have recently been performed on the single-crystal BSCCO which reveal clear evidence for flux-lattice melting in the region of the irreversibility-line, and are described below (7). This material was chosen because of its high anisotropy ($\gamma$ > 100), which causes the melting-line to occur well below the upper-critical field $H_{C2}(T)$.

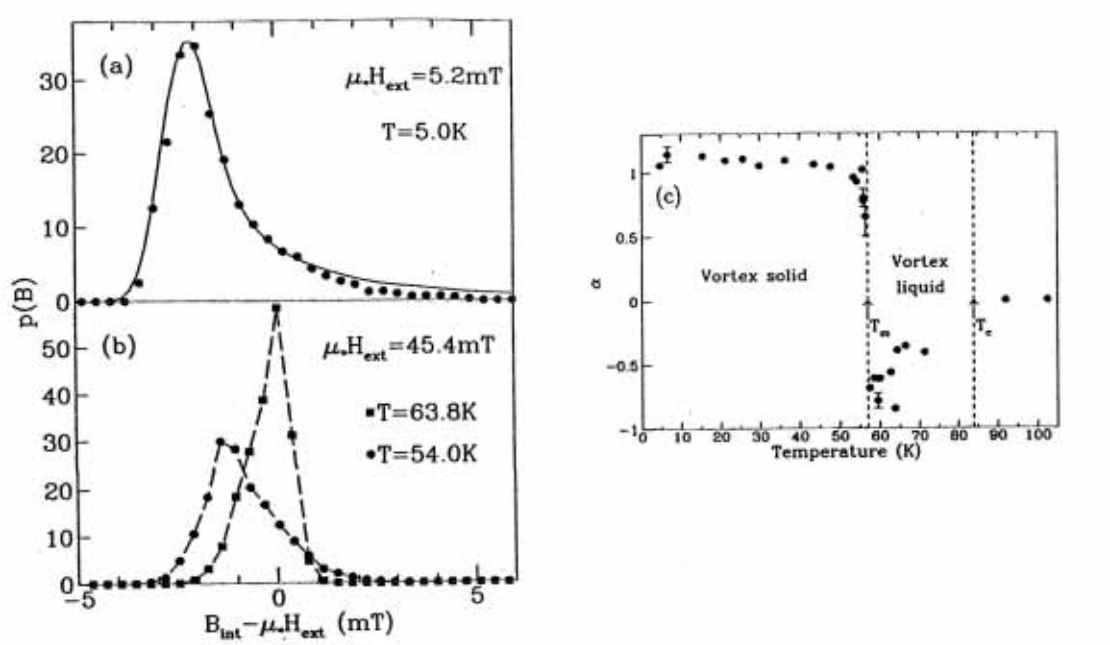


Figure 5: The probability distribution of the internal magnetic fields in $Bi_{2.15}Sr_{1.85}CaCu_2O_{8+\delta}$: (a) At $\mu_0H_{ext}$=5.2mT and T=5.0K, (b) At $\mu_0H_{ext}$=45.4mT, for (i) T=54.0K (circles), (ii) At T=63.8K (squares), just below and above the irreversibility line respectively (7). (c) The temperature dependence of the lineshape asymmetry parameter $\alpha=(\langle\Delta B^3\rangle^{1/3}/\langle\Delta B^2\rangle^{1/2})$ (see text) .

In Fig.5(a) is shown the lineshape taken at 5K after field-cooling the BSCCO single-crystals in a field of 50mT. This has the characteristics of a vortex-line lattice, notably the long high-field tail as discussed in Section 2. In Fig.5(b) are shown lineshapes measured at two temperatures after cooling in 45.4mT, one above and one below the irreversibility-line. The lineshape measured below the line again has characteristics of a vortex-line lattice, while that taken above has a completely different probability distribution; in particular, the long high-field tail is no longer present. This latter lineshape cannot be described in

terms of a static vortex-line solid, and its features are not incompatible with those of a vortex liquid: Such changes of lineshape may be quantified by defining a parameter derived from the third and second moments of the lineshape $\alpha=\langle\Delta B^3\rangle^{1/3}/\langle\Delta B^2\rangle^{1/2}$. This is a dimensionless measure of the asymmetry of the distribution, changes of which reflect changes of the vortex structure. This parameter is plotted in Fig. 5(c) as a function of temperature, and shows a clear indication of a sharp transition of the vortex structure. The field dependence of this transition has also been measured and is as expected for the melting of a vortex-line lattice. Furthermore, the melting-line $B_m(T)$ is found to closely coincide with the irreversibility-line $B_{irr}(T)$. These results have also been confirmed by neutron scattering measurements from the vortex-lattice (35). However, the $\mu^+$SR results are unique in being able to provide information about the vortex structure within the liquid phase, where the neutron signal becomes unobservable due to the lack of long range order.

## 6. Summary

The $\mu^+$SR technique is a unique probe of the probability distribution p(B) of the internal magnetic fields in the mixed state of a type-II superconductor. Measurements of the second moment $\langle\Delta B^2\rangle$ of p(B) can be used to measure the penetration depth $\lambda$ in HTC systems, provided care is taken in the interpretation of the data. The temperature dependence of $\lambda$ may yield information concerning the symmetry and strength of the superconducting pairs, while the observation of universal trends in A within and between families of HTC materials may also provide important information concerning the microscopic behaviour. The measurement of p(B) can also be used to gain information about the microscopic vortex structure in the mixed state, and of flux-vortex phase transitions. Among other things this has recently been used to observe flux-lattice melting in BSCCO.

Although restrictions of space have allowed only a rather narrow review of the applications of $\mu^+$SR to HTC research, I hope that I have been able give some impression of the importance of the technique to this field. It seems certain that in future $\mu^+$SR research will continue to play a key role in this area.

## Acknowledgements

I would like to acknowledge the invaluable collaboration of R. Cubitt, E.M. Forgan, C.E. Gough, H. Keller, P.H. Kes, T.W. Li, A.A. Menovsky, I.M. Savid, R. Schauweeker, T. Schneider, Z. Tarnawski, M. Warden, D. Zech, and P. Zimmermann. This work was supported by the Swiss National Science Foundation (NFP30 Nr. 4030-32785), the Science and Engineering Research Council of the United Kingdom, and by a special grant from the BritishfSwiss Joint Research Programme.

## References

[1] See e.g. Muon Spin Rotation Spectroscopy: Principles and Applications in Solid State

Physics (Adam Hilger, Bristol 1985).

[2] See e.g. Proceedings of the 5th International Conference on Muon Spin Rotation, Relaxation

and Resonance, Oxford, U.K., Hyperfine Interactions 63-65 (1990).

[3] D.S. Fisher, M.P.A. Fisher and D.A. Huse, Phys. Rev. B 43, 130 (1991).

[4] M. Tinkham, Introduction to Superconductivity (McGraw-Hill, New York 1975).

[5] E.H. Brandt, J. Low. Temp. Phys., 73, 355 (1988).

[6] D. Herlach et al., Hyperfine Interactions 63, 41 (1990).

[7] S.L. Lee et al., Phys. Rev. Lett. 71, 3862 (1993).

[8] J. Rammer, Europhys. Lett. 5, 77 (1988).

[9] J. Annett, N. Goldenfeld and S.R. Renn, Phys. Rev. B 43, 2778 (1991).

[10] P. Pincus et al., Physics Letters 13, 21 (1964).

[11] E.H. Brandt, Phys. Rev. B 37, 2349 (1988).

[12] W. Barford and J.M.F. Gunn, Physica C 156, 515 (1988).

[13] S.L. Thiemann, Z. Radovid and V.G. Kogan, Phys. Rev. B 39, 11406 (1989).

[14] E.M. Forgan et al., Hyperfine Interactions 63, 71 (1990).

[15] V.I. Fesenko, V.N. Gorbunov and V.P. Smilga, Physica C 176, 551 (1991).

[16] R. Cubitt et al., Physica C 213, 126 (1993).

[17] M. Weber et al., Phys. Rev. B 48, 13022 (1993).

[18] Y.-Q. Song et al., Phys. Rev. Lett. 70, 3127 (1993).

[19] J.R. Clem, Phys. Rev. 43, 7837 (1991).

[20] E.H. Brandt, Phys. Rev. Lett. 66, 3213 (1991).

[21] D.R. Harshman et al., Phys. Rev. B 47, 2905 (1993).

[22] D.R. Harshman et al., Phys. Rev. Lett. 67, 3152 (1991).

[23] B. Piimpin et al., Journal of the Less-Common Metals 164 & 165, 994 (1990).

[24] H. Keller et al., Physica C 185-189 1089 (1991).

[25] P. Zimmermann et al., Physik-Institut der Universitilt Ziirich, Private communication

(1993).

[26] T. Schneider and H. Keller, Phys. Rev. Lett. 69, 3374 (1992).

[27] Y.J. Uemura et al., Phys. Rev. Lett. 62, 2317 (1989); Y.J. Uemura et al., Phys. Rev. B

38, 909 (1988); Y.J. Uemura et al., Phys. Rev. Lett. 66, 2665 (1991).

[28] T. Schneider and H. Keller, Physica C 207, 366 (1993).

[29] Ch. Niedermayer et al., Phys. Rev. Lett. 71, 1764 (1993).

[30] Y.J. Uemura et al., Nature 364, 605 (1993).

[31] T. Schneider and M.H. Pedersen, submitted for publication (1993).

[32] A. Houghton, R.A. Pelcovits, and A. Sudbe, Phys. Rev. B 40, 6763 (1990).

[33] E.H. Brandt, Phys. Rev. Lett. 63, 1106 (1989).

[34] L.I. Glazman and A.E. Kosheley, Phys. Rev. B 43, 2835 (1991).

[35] R. Cubitt et al., Nature 365, 407 (1993).

[36] R.G. Beck et al., Phys. Rev. Lett. 68, 1594 (1992).

[37] H. Safar et al., Phys. Rev. Lett. 70, 3800 (1993).

[38] A. Schilling et al., Phys. Rev. Lett. 71, 1899 (1993).

[39] P.L. Gammel et al., Phys. Rev. Lett. 61, 1666 (1988).